Journal of Mammary Gland Biology and Neoplasia (2018) 23:89–99
https://doi.org/10.1007/s10911-018-9396-0

Radiological, Histological and Chemical Analysis of Breast Microcalcifications: Diagnostic Value and Biological Significance

Rita Bonfiglio[1] · Manuel Scimeca[2,3,4] · Nicola Toschi[4,5,6] · Chiara Adriana Pistolese[4] · Elena Giannini[1] · Chiara Antonacci[1] · Sara Ciuffa[1] · Virginia Tancredi[3,7] · Umberto Tarantino[8] · Loredana Albonici[9] · Elena Bonanno[1,10]

Received: 7 December 2017 / Accepted: 3 May 2018 / Published online: 9 May 2018

Abstract

Classification of mammary microcalcifications is based on radiological and histological characteristics that are routinely evaluated during the diagnostic path for the identification of breast cancer, or in patients at risk of developing breast cancer. The main aim of this study was to explore the relationship between the imaging parameters most commonly used for the study of mammary microcalcifications and the corresponding histological and chemical properties. To this end, we matched the radiographic characteristics of microcalcifications to breast lesion type, histology of microcalcifications and elemental composition of microcalcifications as obtained by energy dispersive x ray (EDX)-microanalysis. In addition, we investigated the properties of breast cancer microenvironment, under the hypothesis that microcalcification formation could result from a mineralization process similar to that occurring during bone osteogenesis. In this context, breast lesions with and without microcalcifications were compared in terms of the expression of the main molecules detected during bone mineralization (BMP-2, BMP-4, PTX3, RANKL OPN and RUNX2). Our data indicate that microcalcifications classified by mammography as "casting type" are prevalently made of hydroxyapatite magnesium substituted and are associated with breast cancer types with the poorest prognosis. Moreover, breast cancer cells close to microcalcifications expressed higher levels of bone mineralization markers as compared to cells found in breast lesions without microcalcifications. Notably, breast lesions with microcalcifications were characterized by the presence of breast-osteoblast-like cells. In depth studies of microcalcifications characteristics could support a new interpretation about the genesis of ectopic calcification in mammary tissue. Candidating this phenomenon as an integral part of the tumorigenic process therefore has the potential to improve the clinical management of patients early during their diagnostic path.

Keywords Microcalcifications · Breast cancer · Osteoblast-like cells · Casting type · RUNX2 · RANKL · BMPs · PTX3

Rita Bonfiglio, Manuel Scimeca and Nicola Toschi equally contributed to this work

✉ Elena Bonanno
elena.bonanno@uniroma2.it

Manuel Scimeca
http://www.orchidealab.it

[1] Department of Experimental Medicine and Surgery, University of Rome Tor Vergata, Via Montpellier 1, 00133 Rome, Italy

[2] OrchideaLab S.r.l., via del Grecale 6, Morlupo, Rome, RM, Italy

[3] IRCCS San Raffaele Pisana, 00166 Rome, Italy

[4] Department of Biomedicine and Prevention, University of Rome "Tor Vergata", Via Montpellier 1, 00133 Rome, Italy

[5] Martinos Center for Biomedical Imaging, Boston, MA, USA

[6] Harvard Medical School, Boston, MA, USA

[7] Department of Systems Medicine, School of Sport and Exercise Sciences, University of Rome Tor Vergata, Rome, Italy

[8] Department of Orthopedics and Traumatology, "Tor Vergata" University of Rome, "Policlinico Tor Vergata" Foundation, Rome, Italy

[9] Department of Clinical Sciences and Translational Medicine, University of Rome "Tor Vergata", 00133 Rome, Italy

[10] IRCCS Neuromed Lab. 'Diagnostica Medica' & 'Villa dei Platani', 83100 Avellino, Italy

Abbreviation

HA	Hydroxyapatite
CO	Calcium oxalate
EDX	Energy dispersive x-ray
Mg-HAp	Magnesium-substituted hydroxyapatite
H & E	Hematoxylin and eosin
BMP-2	Bone morphogenic protein-2
BMP-4	Bone morphogenic protein-4
PTX3	Pentraxin 3
RUNX2	Runt-related transcription factor 2
RANKL	Receptor activator of nuclear factor kappa-B ligand
VDR	Vitamin d receptor
OPN	Osteopontin
GLMs	General linear models
WHO	World health organization
BL	Benign lesion
ML	Malignant lesion
BLm	Benign lesion with microcalcifications
MLm	Malignant lesion with microcalcifications
Re. Co. M.N.	Reporting and codifying the results of mammography
BOLCs	Breast osteoblast-like cells

Introduction

Several major pathological conditions (e.g. cardiovascular diseases and cancer) display mineral or organic compound deposition [1]. Tissue calcifications are defined as the deposition of calcium salts, along with smaller amounts of iron, magnesium, and other mineral salts [1].

In breast tissues, the presence of microcalcifications plays a crucial role in early cancer diagnosis [2]. Indeed, approximately 50% of non-palpable breast cancers are detected by mammography exclusively through the study of microcalcification patterns [3], and this approach is able to reveal up to 90% of in situ ductal carcinoma cases [4]. Currently radiologists employ three distinct classification systems/scales for the diagnostic and prognostic evaluation of breast microcalcifications: Madame Le Gal, BI-RADS and Re.Co.R.M [4, 5].

These systems are based on estimating the statistical risk of developing breast cancer based on the appearance of microcalcifications on the mammogram. This assessment is mainly based on morphology, but also on distribution, site, dimension and number of microcalcifications. In addition, previous studies have suggested an association between physical and chemical properties of microcalcifications and patient prognosis [6].

Historically, the chemical composition of microcalcification is related to two main types of calcium deposits: calcifications of calcium oxalate (CO), and calcifications of calcium phosphate, mainly hydroxyapatite (HA) [6]. In this context, previous studies have observed that calcium oxalate calcifications are often associated with benign lesions, whereas hydroxyapatite calcifications are related both to benign and malignant lesions [6–8]. In a recent paper, we demonstrated for the first time the existence of a new subtype of hydroxyapatite in breast cancer calcifications: magnesium-substituted hydroxyapatite (Mg-Hap). Interestingly, Energy Dispersive X-Ray (EDX) –microanalysis revealed that Mg-HAp calcifications appeared in conjunction with malignant lesions exclusively [7]. Recent discoveries in the field of the biology of breast and prostate calcifications demonstrated the presence of cells capable to produce calcified crystals [7, 9]. In addition, our and other studies showed that only the complex form of calcification (HA and Mg-HAp) were produced by these cells (osteoblast-like cells) [7]. Based on these considerations, the simultaneous study of the morphology of calcifications (both at the histological and at the radiological level) and the process of their formation it is essential for a full understanding of the role of microcalcifications in breast cancer. Moreover, the combination of these data can provide the rationale for the development of new tools for early detection of calcifications that are actively produced by osteoblast like cells through a process similar to physiological mineralization discriminating them from those formed by cancer degenerative processes.

Therefore, the main aim of this study was to establish a correlation between the detection of the most commonly used imaging parameters for the study of mammary microcalcifications and the corresponding histological and chemical properties. To this end, we matched the radiographic characteristics of microcalcifications to the following data: breast lesion type, histology of microcalcifications and elemental composition of microcalcifications as obtained by energy dispersive x ray (EDX)-microanalysis. In addition, we investigated the properties of breast cancer microenvironment, under the hypothesis that microcalcification formation could result from a mineralization process similar to that occurring during bone osteogenesis. Thus, breast lesions with microcalcifications and lesions without microcalcifications were compared in regard to the expression of the main molecules detected during bone mineralization (BMP-2, BMP-4, PTX3, RANKL OPN and RUNX2).

Materials and Methods

Breast Sample Collection

For this study we retrospectively collected 110 paraffin embedded diagnostic blocks from breast biopsies performed during the period December 2011–December 2013 at Policlinico Tor Vergata. From each paraffin-embedded block, serial sections were obtained to perform histological classification and immunohistochemical analysis. In addition, 1 mm^3 tissue

fragments were used to perform ultrastructural (transmission electron microscopy) and microanalytical (EDX-microanalysis) investigations. This study protocol was approved by the "Policlinico Tor Vergata" Independent Ethical Committee (reference number # 94.13).

Radiological Examination

The radiological images were blindly and independently interpreted by 2 radiologists. The lesions were analyzed using the criteria proposed by a) the BI-RADS USdx [10] (based on shape, margins, echotexture, posterior acoustic features, and the relationship to adjacent tissues lesions were classified into categories 2, 3, 4, and 5), b) the Le Gal' score [11] and c) Re.Co.R.M classification system [12]. Microcalcifications were analyzed blindly and independently by 2 radiologists according to the classification of Tabár et al. 2005 [13].

Histology

After fixation in 10% buffered formalin for 24 h, breast tissues were embedded in paraffin. Three-micrometer thick sections were stained with hematoxylin and eosin (H & E) and the diagnostic classification was blindly performed by two pathologists [14].

Immunohistochemistry

Immunohistochemical analysis was performed to assess the expression of the following mineralization factors: RUNX2, Bone Morphogenic Protein-2 (BMP-2), Bone Morphogenic Protein-4 (BMP-4), RANKL, osteopontin (OPN), Pentraxin-3 (PTX3).

Briefly, 4-μm thick sections from diagnostic blocks were pre-treated with EDTA citrate pH 7.8 for 30 min at 95 °C and then incubated with the following antibodies: rabbit monoclonal anti-OPN (clone N/A; Novus Biologicals, Littleton, CO, USA; 1:100 diluted) and mouse monoclonal anti-RANKL (clone 12A380; Abcam, Cambridge, UK; 1:100 diluted).

In order to perform immunostainings for BMP-2, BMP-4, RUNX2 and PTX3, 4-μm-thick sections were pre-treated with Citrate pH 6.0 for 30 min at 95 °C and then incubated, respectively, with rabbit monoclonal anti-BMP-2 (clone N/A; Novus Biologicals, Littleton, CO, USA; 1:500 diluted) [15], rabbit monoclonal anti-BMP-4 (clone 6B7 Novus Biologicals, Littleton, CO, USA; 1:250 diluted) and rat polyclonal anti-PTX3 (clone MNB1; Abcam, Cambridge, UK diluted 1:100) antibodies. Washings were performed with PBS/Tween20 pH 7.6 (UCS diagnostic, Rome, Italy); reactions were revealed by HRP - DAB Detection Kit (UCS diagnostic). Immunohistochemical positivity was evaluated on digital images (Iscan Coreo, Ventana, Tucson, AZ, USA) by a semi-quantitative approach. Specifically, immunoreaction was evaluated by counting the number of positive breast cells out of a total of 500 in randomly selected regions. To assess the background of immuno-staining, we included a negative control for each reaction by incubating the sections with secondary antibodies (HRP) and detection system (DAB). According to the data sheets, reactions have been set-up by using specific control tissues.

Energy Dispersive x-Ray (EDX) Microanalysis

All breast samples underwent ultrastructural microanalysis. Following to the identification of microcalcifications, six-micrometer-thick paraffin sections were embedded in Epon resin as previously described [16]. Briefly, sections were de-paraffinized, hydrated, osmium tetroxide-fixed, dehydrated in ethanol and propylene oxide and infiltrated in Epon. The embedding capsules were positioned over areas containing microcalcifications identified by Toluidine Blue staining previously. Unstained ultra-thin sections of approximately 100-nm-thick were mounted on copper grids for semi-quantitative microanalysis. EDX spectra of microcalcifications were acquired with a Hitachi 7100FA transmission electron microscope (Hitachi, Schaumburg, IL, USA) and an EDX detector (Thermo Scientific, Waltham, MA, USA) at an acceleration voltage of 75 KeV and magnification of 12.000. Spectra were semi-quantitatively analyzed by the Noram System Six software (Thermo Scientific, Waltham, MA, USA) using the standardless Cliff-Lorimer k-factor method [16–18]. The EDX microanalysis apparatus was calibrated using an x-ray microanalysis standard (Micro-Analysis Consultants Ltd., Cambridgeshire, UK). Microanalytical data are reported in terms of presence/absence of each chemical element detected in the selected area. According to the spectra detected in correspondence of calcifications they were classified as: a) calcium oxalate calcifications, when spectra showed the simultaneous presence of Calcium, Oxygen and Carbon, b) hydroxyapatite calcifications, when spectra showed the simultaneous presence of Calcium, Phosphate and Carbon and c) Hydroxyapatite Magnesium-substituted calcifications, when spectra showed the simultaneous presence of Calcium, Phosphate and Magnesium.

Statistical Analysis

Separate x^2 tests were used to assess the associations between radiological appearance and elemental composition, between malignancy and elemental composition and between morphological appearance and elemental composition. Separate General Linear Models (GLMs) were used to assess the association between immunohistochemical data (BMP-2, BMP-4, PTX3, OPN, RANKL, RUNX2) as dependent variables and the following pairs of categorical independent factors:

(Malignancy / Presence of Microcalcification), (Malignancy / Histological Appearance), (Malignancy / Elemental Composition), (Malignancy / Radiological Appearance). For every pair of factors, a first-order interaction term was also included in each model. Whenever a significant effect of a categorical factor, of the interaction term or of both was observed, between-level *post-hoc* comparisons were performed through the LSD test. Additionally, a separate set of univariate GLMs were used to assess the association between radiological classification scores (Madame Le Gal, BI-RADS and Re.Co.R.M) as dependent variables and the following categorical factors: Elemental Composition, Histological Appearance. Again, whenever a significant effect of a categorical factor was found, between-level *post-hoc* comparisons were performed through the LSD test. Statistical analysis was performed using SPSS Statistics v23.

Results

Histology

The study of H&E sections allowed us to classify breast biopsies according to WHO 2012 [19] into benign lesions (BL, $n = 44$) and malignant lesion (ML, $n = 66$). BL and ML lesions were further classified according to the presence/absence of microcalcifications. BL without microcalcifications (BL, $n = 20$) were all fibrocystic mastopathies, whereas among BL presenting microcalcifications (BLm, $n = 24$) were identified 14 fibrocystic mastopathies and 10 fibroadenomas. Among ML, lesions without microcalcifications (ML, n = 20) were all classified as infiltrating ductal carcinomas (ICm), whereas lesions presenting microcalcifications (MLm, $n = 46$) were identified as infiltrating ductal carcinomas (ICm, $n = 23$) and ductal in situ carcinomas (ISCm, n = 23).

Histological Appearance of Microcalcifications

Under light microscopy, microcalcifications appeared in three distinct forms: polymorphous bodies, birifrangent crystals, psammoma bodies. Polymorphous bodies were found both in BLm (6 fibrocystic mastopathies and 4 fibroadenomas) and in MLm (14 ISCm and 22 ICm) whereas birifrangent crystals were detected only in BLm (8 fibrocystic mastopathies and 6 fibroadenomas). Psamomma bodies were detected only in MLm (9 ISCm and 1 ICm).

Association between Elemental Composition and Histology

Ultrastructural elemental microanalysis performed on breast microcalcifications confirmed the presence of the previously known types of calcifications: CO, HA and Mg-HAp (Fig.1). The χ^2 test showed a significant association between elemental composition and malignancy ($p < .00001$). Specifically, the presence of CO coincided with benign lesions in 100% of cases, whereas complex forms of microcalcifications (HA and Mg-HAp) were exclusively found in malignant lesions.

Of note, among the total number of cancerous lesions with microcalcifications made of Mg-HAp, 46% of them corresponded to lesions from in situ carcinoma of high grade.

Also, the x^2 test showed a significant association between the type of calcification and histological classification ($p < 0.001$). Specifically, CO microcalcifications appeared as unstained birefringent crystals in 79% of cases and as polymorphous bodies in 21% of cases; among the 24 HA microcalcifications, 29% were classified as 7 psammoma bodies whereas 71% were defined as polymorphous bodies. Among the totality of Mg-HAp microcalcifications, 96% appeared as polymorphous bodies and 4% was classified as psammoma bodies.

Association between Elemental Composition and Mammographic Morphological Appearance

Microcalcifications detected by digital mammography showed the following forms: powdery, casting type, rounded, crushed stones, mixed (Fig.2a–c).

Interestingly, the x^2 test showed a significant association between morphological appearance and elemental composition ($p < 0.001$). In particular, CO microcalcifications appeared as 43% mixed, 43% rounded and 14% powdery (Fig.2a), HA microcalcifications were 33% casting type, 25% mixed, 17% crushed stones, 17% powdery and 8% rounded (Fig.2b), whereas Mg-HAp microcalcifications were 69% casting type, 15% crushed stones, 8% powdery and 8% mixed (Fig.2c). Additionally, GLM analysis revealed a significant effect of elemental composition on all three classification systems (Madame Le Gal: $p < 0.001$, BI-RADS: $p < 0.001$, Re.Co.R.M: $p < 0.001$) (Fig.2d–f). Specifically, we found higher mean Madame Le Gal scores in lesions with Mg-HAp (4.15 ± 0.17) with respect to both lesions with CO (2.833 ± 0.21) or HA (3.08 ± 0.18) (post-hoc comparisons: CO vs HA $p = 6260$; CO vs Mg-HAp $p < 0.001$; HA vs HAp $p = 0.001$) (Fig.2d). We found a similar pattern with the BI-RADS system (CO 2.79 ± 0.20; HA 2.90 ± 0.16; Mg-HAp 3.89 ± 0.17; post-hoc comparisons: CO vs HA p=; CO vs Mg.HAp $p < 0.001$; HA vs Mg-HAp $p = 0.0002$) (Fig.2e). A different pattern was seen when using Re.Co.R.M. scores (HA 2.54 ± 0.14; HA 3.40 ± 0.15; Mg-HAp 3.75 ± 0.16), and in this case post hoc testing found no significant differences Re.Co.R.M. scores between HA and Mg-HAp ($p = 0.1674$) (Fig. 2f). On the other hand, significant differences in Re.Co.R.M. scores were observed between both CO and HA ($p = 0.0003$), and CO and Mg-HAp ($p < 0.001$) (Fig. 2f).

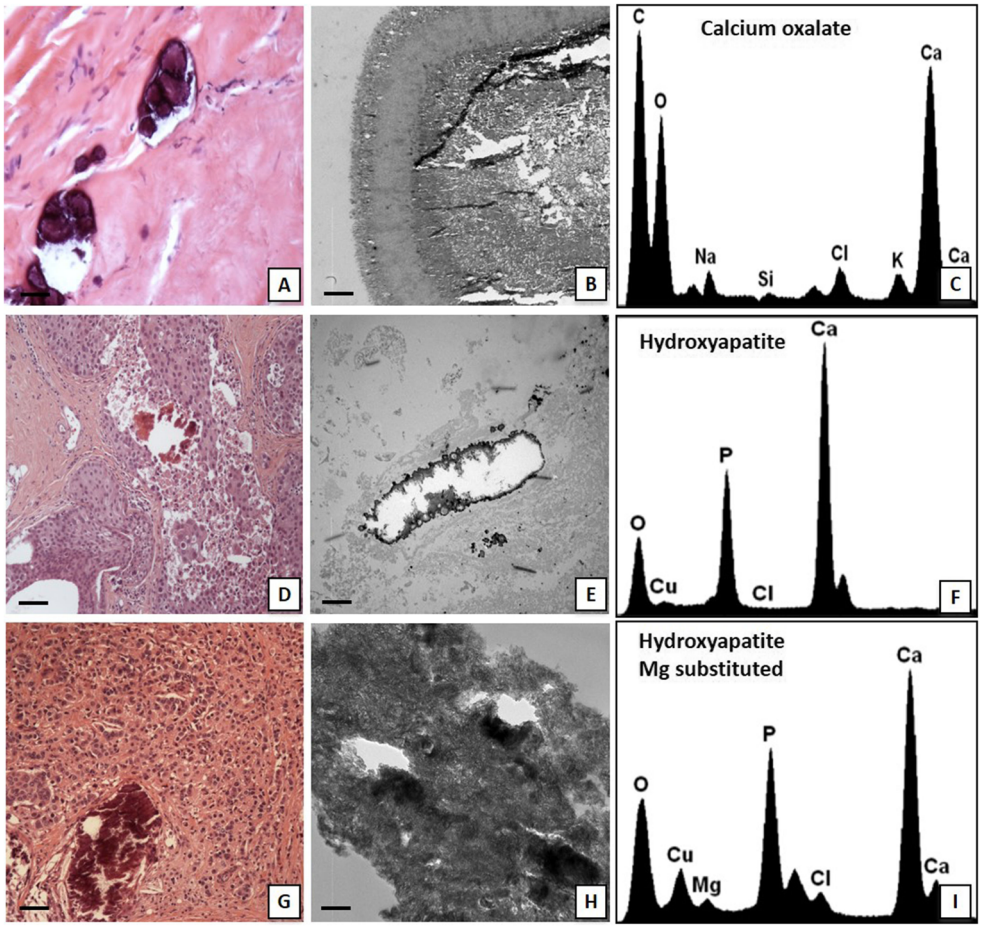

Fig. 1 Elemental composition of calcification in breast pathology. Benign lesion showing psamomatous calcifications (**a** haematoxylin eosin stain; **b** TEM micrograph) composed of calcium oxalate (**c** EDX spectrum). Malignant lesion showing amorphous calcifications (**d** and **g** haematoxylin eosin stain; E and H TEM micrographs) composed of hydroxyapatite (**f** EDX spectrum) or hydroxyapatite Mg substituted (**i** EDX spectrum). **a**, **d**, **g** scale bar represent 50 μm. **b**, **h** scale bar represent 0,2 μm (**e**) scale bar represent 1 μm

Mineralization Process in Breast Lesions

Immunoistochemical positivity was evaluated on digital images (Iscan Coreo, Ventana, Tucson, AZ, USA) by a semi-quantitative approach.

We found a significant effect of both malignancy ($p < 0.001$, ML > BL) and the presence of microcalcifications ($p < 0.001$: lesions with microcalcifications>lesions without microcalcifications) on BMP-2, while the interaction term was borderline significant ($p = 0.057$) (Fig. 3a–d). Post-hoc testing revealed significant differences both between BL and BLm (BL 72.39 ± 18.46, BLm 139.4 ± 13.51, $p = 0.0010$) and between ML and MLm (ML 116.9 ± 12.9, MLm 314.15 ± 40.45, $p < 0,0001$) (Fig. 3a–e). We also found a significant effect of both malignancy ($p < 0.036$) and the presence of microcalcifications ($p < 0.006$) on the rate of BMP-4 positive breast cells ($p = 0.0026$) (Fig. 3f–j). The interaction term was not significant. In accordance with what was observed in terms of BMP-2, post-hoc testing showed a significantly higher rate of BMP-4 expression in BLm (134.0 ± 17.31) and MLm (175.7 ± 12.84) as compared with BL (71.50 ± 17.47) and ML (139.3 ± 14.13), respectively (BL vs BLm, $p = 0.0200$; ML vs MLm, $p = 0.0046$) (Fig. 3f–j).

Immunostaining for PTX3 also revealed a significant effect of both malignancy ($p < 0.001$) and the presence of microcalcifications ($p < 0.001$) (Fig. 3k–o). The interaction term was also significant ($p = 0.035$: $(ML\text{-}BL)_{micro} > (ML\text{-}BL)_{nomicro}$), indicating that the difference in PTX3 expression between malignant and benign lesions is significantly greater in the presence of microcalcifications as compared to the same difference in absence of microcalcifications. In post-hoc testing, a significantly higher rate of PTX3 positive breast cells was found in MLm as compared with ML (MLm 299.3 ± 21.51, ML 166.2 ± 17.58, MLm vs ML $p < 0.0001$) (Fig. 3k–o). Moreover, we observed significant differences in PTX3 expression between BLm and ML ($p = 0.0314$), BLm and Mlm ($p < 0.0001$), BL and MLm ($p < 0.0001$). No difference in PTX3 expression was observed when comparing BL with and without microcalcifications (BL 108.6 ± 18.90, BLm 114.3 ± 14.08, BL vs BLm $p = 0.6853$) (Fig. 3k–o).

We also found a significant effect of both malignancy ($p < 0.001$, BL > ML) and the presence of microcalcifications ($p < 0.001$ lesions with microcalcifications > lesions without microcalcifications) in nuclear expression of RUNX2 (Fig. 4a–e). The interaction term was not significant. Post-hoc testing revealed significant differences between BL and MLm

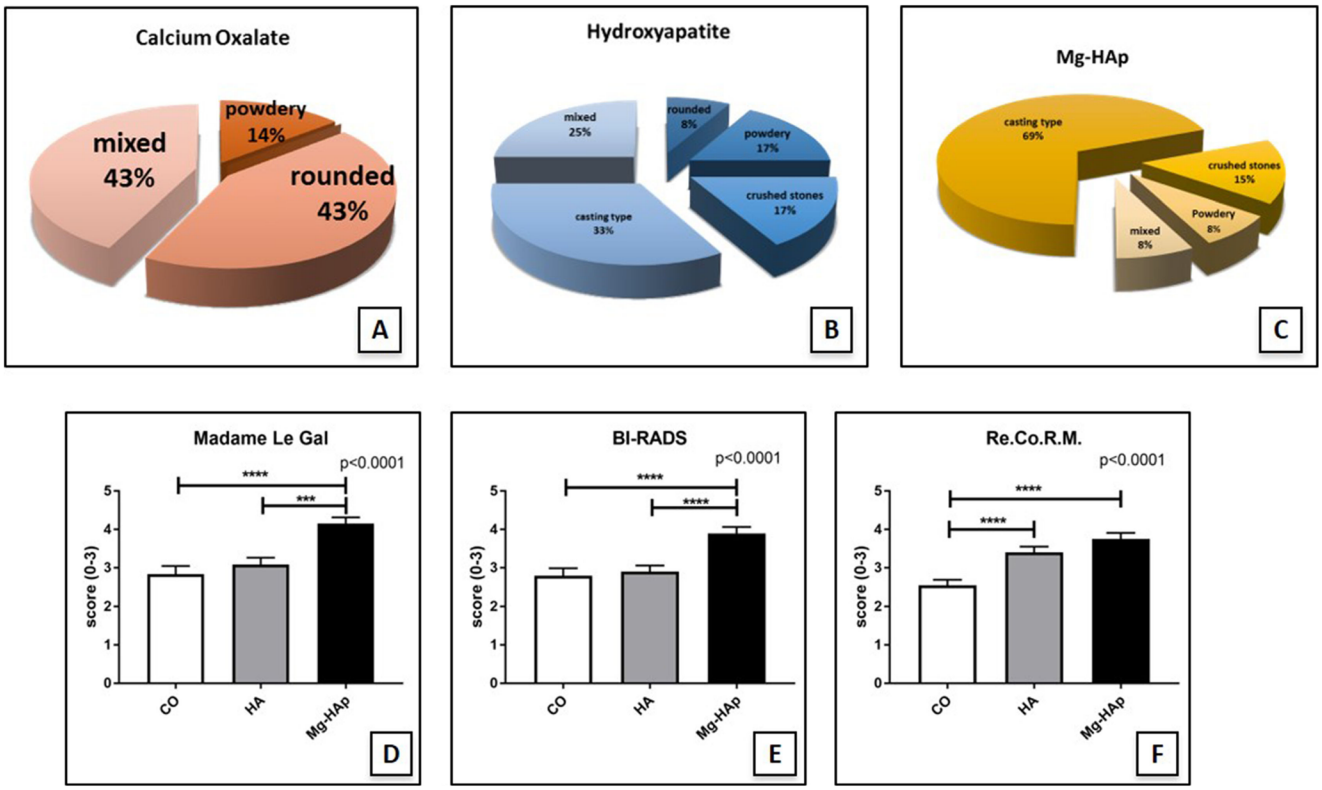

Fig. 2 Radiological and EDX data of breast microcalcifications. a Radiological aspect of breast microcalcifications made of CO (**b**) Radiological aspect of breast microcalcifications made of HA. **c** Radiological aspect of breast microcalcifications made of Mg-HAp (**d**, **e**, **f**) According to the classifications of Madame Le Gal, BI-RADS and Re.Co.R.M, Mg-HAp microcalcifications consistently showed an higher risk of breast cancer in comparison to CO and HA microcalcifications

($p < 0.0001$), BLm and MLm ($p = 0.0016$) and ML and MLm ($p = 0.0003$). (Fig. 4a–e).

In addition, we found a significant effect of both malignancy ($p < 0.0001$, BL > ML) and the presence of microcalcifications ($p = 0.005$ lesions with microcalcifications> lesions without microcalcifications) on RANKL expression (Fig. 4f–j). The interaction term was not significant. Post-hoc testing detected significantly higher RANKL signal in BLm (170.8 ± 32.05) with respect to BL (88.95 ± 11.55) ($p = 0.0364$). Also, we detected significant differences between BL and ML ($p = 0.0014$), BL and MLm ($p < 0.0001$), BLm and MLm ($p = 0.0030$) (Fig. 4f–j). Interestingly, RANKL positive breast cells were frequently found close to microcalcifications and they morphologically resemble to osteoblast cells (Fig. 4j). No significant differences ($p = 0.3395$) were found by comparing ML with (269.7 ± 22.9) or without (228.8 ± 36.62) microcalcifications.

Finally, we found a significant effect of both malignancy ($p < 0.001$, ML > BL) and the presence of microcalcifications ($p < 0.001$ lesions with microcalcifications > lesions without microcalcifications) on the rate of OPN positive breast cells (Fig.4k–o). The interaction term was not significant. In line with BMP-2 and BMP-4 expression, post-hoc testing revealed significant differences between BL and BLm (BL 66.56 ± 18.04, BLm 165.6 ± 17.99, BL vs BLm $p < 0.0001$), ML and MLm (ML 151.9 ± 16.59, MLm 219.3 ± 22.9, ML vs MLm $p = 0.0104$), BL and MLm ($p = 0.0001$) (Fig. 4k–o).

Fig. 3 Expression of bone mineralization inductors in breast cells. ▶ Immunohistochemical positivity was evaluated on digital images by a semi-quantitative approach. Specifically, immunoreaction BMP-2, BMP-4, PTX3 was evaluated by counting the number of positive breast cells out of a total of 500 in randomly selected regions. **a** The graph shows the results for BMP-2 immunostaining. **b** Low expression of BMP-2 in a breast benign lesion. **c** Several BMP-2 positive breast cells close to microcalcification (arrow head) in a benign lesion. **d** Ductal in situ carcinoma characterize by both positive and negative BMP-2 breast cancer cells. **e** Ductal in situ carcinoma with a microcalcification (arrow head). All breast cancer cells next to microcalcification express BMP-2. **f** The graph shows the results for BMP-4 immunostaining. **g** Rare BMP-4 positive breast cells in a benign lesion. **h** Intraductal microcalcification (arrow heads) surrounded by BMP-4 positive breast cells in a benign lesion. **i** BMP-4 immunostaining in a ductal in situ carcinoma. **j** BMP-4 positive breast cancer cells close to microcalcification in a ductal in situ carcinoma arrow head). **k** The graph shows the results for PTX3 immunostaining. **l** Image shows rare PTX3 positive cells in a breast benign lesion. **m** Numerous PTX3 positive cells next to microcalcifications arrow heads) in a benign lesion of the breast. **o** Ductal in situ carcinoma characterize by both negative and positive PTX3 cancer cells. **p** All breast cancer cells next to microcalcification express PTX3 (arrow heads). horizontal bars in the graphs represent significant differences (*$p < 0.05$; **$p < 0.01$; ***$p < 0.001$, ****$p < 0.00001$). For each image scale represent 80 μm

Discussion

Microcalcifications play a crucial role in early diagnosis of breast cancer [2]. Approximately 50% of non-palpable breast cancers are detected by mammography exclusively through microcalcification patterns [3], and this approach is able to reveal up to 90% of ductal carcinomas in situ [4].

Improving the characterization of microcalcifications would therefore turn these early signs of breast cancer into even more accurate diagnostic and prognostic markers useful in clinical practice.

To this end, in this study we investigated the associations among the radiological characteristics of microcalcifications, their microscopic appearance and their chemical composition.

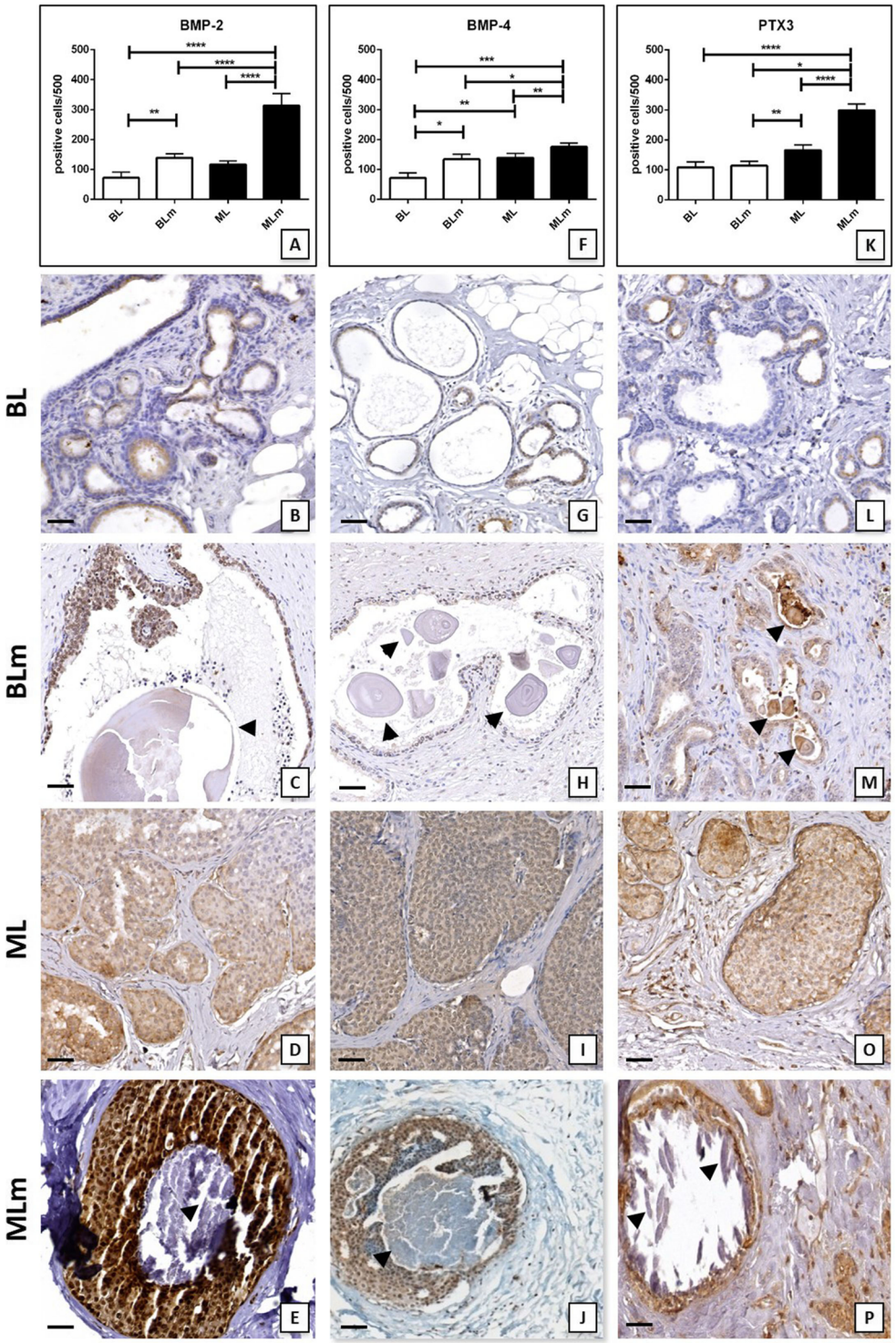

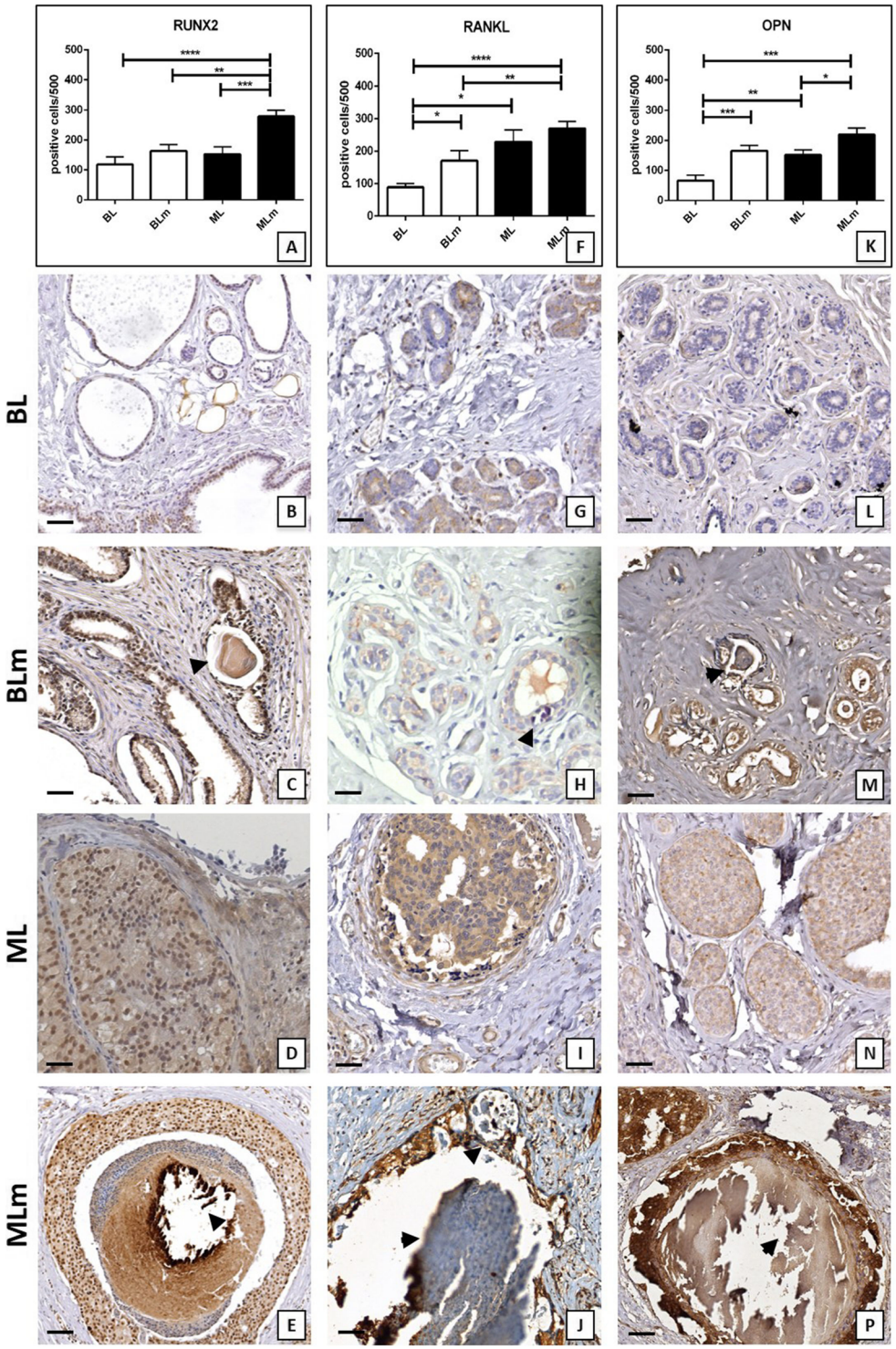

EDX microanalysis confirmed previous data about the presence and distribution of CO, HA and Mg-HAp in breast tissues [7, 20]. In particular, we verified that complex forms of calcifications (HA and Mg-HAp) are strictly related to malignant lesions, whereas microcalcifications associated to benign lesions are exclusively made of CO. Conversely, Mg-HAp was never found in benign lesions, and it was frequently detected in breast cancer. Moreover, we found that the elemental composition of microcalcifications was significantly associated with their morphological appearance. Specifically, CO microcalcifications were frequently classified as birefringent crystals, whereas calcification made of Mg-HAp appeared as polymorphous bodies in more than 90% of cases. Accordingly, histological appearance of microcalcifications

◀ **Fig. 4 Expression of osteoblast markers in breast cells.** Immunohistochemical positivity was evaluated on digital images by a semi-quantitative approach. Specifically, immunoreaction RUNX2, RANKL, OPN was evaluated by counting the number of positive breast cells out of a total of 500 in randomly selected regions. **a** The graph shows the results for RUNX2 immunostaining. **b** Rare RUNX2 positive cells in a breast benign lesion. **c** Several RUNX2 positive cells in a benign lesion with microcalcification (arrow head). **d** RUNX2 nuclear expression a ductal in situ carcinoma. **e** All breast cancer cells next to microcalcification express RUNX2 (arrow head). **f** The graph shows the results for RANKL immunostaining. **g** Image displays RANKL expression in a benign lesion without microcalcifications. **h** Numerous positive RANKL cells next to microcalcification (arrow head). **i** Positive breast cancer cells in a ductal in situ carcinoma. **j** RANKL positive breast cancer cells close to microcalcification (arrow head) in a ductal in situ carcinoma. **k** The graph shows the results for OPN immunostaining. **l** Rare/no positive OPN cells in a breast benign lesion. **m** Numerous OPN positive cells next to microcalcifications (arrow head) in a benign lesion of the breast. **n** OPN expression a ductal in situ carcinoma. **p** Intraductal microcalcification (arrow head) surrounded by OPN positive breast cells in a ductal in situ carcinoma. Horizontal bars in the graphs represent significant differences (*$p < 0.05$; **$p < 0.01$; ***$p < 0.001$, ****$p < 0.00001$). For each image scale represent 80 μm

could be considered as a useful prognostic factor for breast lesions.

In this paper, for the first time we analyzed the association between the chemical composition of microcalcifications and their morphological appearance on the mammogram. Notably, microcalcifications made of Mg-HAp were mainly associated to "casting type" classification. In this context, Tabar et al. proposed that "casting type" calcifications could represent both an in situ carcinoma and a "duct forming high grade invasive carcinoma", where cancer cells are situated within the newly formed ducts, mimicking the adjacent in-situ process. This process of neo-ductogenesis appears to account for the significant, potentially harmful portion of the tumor burden [21]. In particular, in this paper, we showed that "casting type" microcalcifications are those prevalently made of Mg-Hap and are therefore associated with breast cancer types with poorest prognosis.

Moreover, we found that both HA and Mg-HAp calcifications corresponded to the highest cancer risk according to the main radiological classification system (Madame Le Gal, BI-RADS and Re.Co.R.M).

The production of complex forms of calcifications (HA and Mg-HAp), which we found in malignant lesions, could be related to an active process of ectopic mineralization [7]. For a long time, microcalcifications were interpreted as a mere degenerative process associated with tumorigenesis [22]. More recently, our and other studies suggest that breast microcalcifications are the result of an active biological process characterized by the deposition of calcium salts, similar to what is well known to occur for the physiological mineralization occurring in bone [23–25]. In accordance with this hypothesis, we aimed to test whether some of the main factors typically involved in bone metabolism are similarly involved in the genesis of complex form of breast microcalcifications. In a previous paper, we evaluated the expression of BMP-2 and OPN in biopsies from patients affected by breast cancer with microcalcifications and we found a significant overexpression of typical markers of bone mineralization in infiltrating carcinomas with microcalcifications as compared to infiltrating carcinomas without microcalcifications [7]. Here we investigated for the first time the expression of BMP-2, BMP-4, PTX3, RUNX2, RANKL and OPN in breast tissue environment by comparing benign and malignant lesions with or without microcalcifications.

BMP-2 is the most important inducer of mineralization in bone tissue and BMP-4 participates in the same process (albeit to a lesser extent) [26]. In particular, these molecules are able to induce osteoblasts differentiation of mesenchymal stem cells by inducing the expression of typical osteoblast markers such as RUNX2. Interestingly, we found a significant increase in the expression of these two typical bone markers in breast lesions with microcalcifications as compared to those without microcalcifications.

Recently, we described PTX3 as a new possible marker of poor differentiated breast carcinomas [27]. In addition, we found that high levels of PTX3 are associated with better bone quality in humans and its functional inhibition in vitro hinder mature osteoblasts in producing HA crystals [15, 28]. In line with these evidences, here we found a significantly higher PTX3 signal in the environment of malignant lesions presenting microcalcifications with respect to malignant lesions without microcalcifications. Also, Lee et al., demonstrated that PTX3 induces the upregulation of RANKL [29], a typical marker of mature osteoblasts [30]. The finding that the difference in PTX3 expression between malignant and benign lesions is significantly greater in the presence of microcalcifications suggests an essential role for PTX3 in the formation of ectopic calcifications in breast. When analyzing the main markers of osteoblasts, we found a significantly higher number of RUNX2 and RANKL positive breast cells in malignant lesions with microcalcifications with respect to benign lesions with or without microcalcifications. Both of these molecules are expressed by cells morphologically similar to osteoblasts and were frequently localized close to psammoma bodies. Specifically, the number of positive RUNX2 cancer cells was higher in malignant lesions with microcalcifications respect to both benign lesions and malignant lesion without microcalcifications. Runx2 is the first transcription factor required for the determination of the osteoblast lineage, inducing the differentiation of multipotent mesenchymal cells into immature osteoblasts and directing the formation of bone matrix [31]. In addition, it is known that the molecules of the BMP family, (i.e. BMP-2) are able to induce osteoblasts differentiation by inducing overexpression of RUNX2 [31]. Thus, the finding of RUNX2-positive breast cells close

to microcalcifications strongly supports the hypothesis that calcium deposits in breast are produced by breast cells with an osteoblast phenotype [7].

The absence of a significant difference in the expression of RANKL between malignant lesions with and without microcalcifications leads us to speculate that the role played by RANKL positive cells could be confined to the early phases of microcalcification production.

The formation of HA crystals during osteogenesis requires the participation of OPN [32]. In accordance with the hypothesis that the genesis of breast microcalcifications mimics the physiological process of mineralization which occurs during bone formation, immunostainings for osteopontin revealed (in both benign and malignant lesions, with or without microcalcifications) that the expression of this molecule is significantly higher in breast lesions presenting microcalcifications as compared to those without them.

Taken together, our data further strengthen the hypothesis that breast microcalcifications are the result of a biological phenomenon orchestrated by cells able to actively produce calcium depositions. These cells present an osteoblast like phenotype [7] and, therefore, have been named breast osteoblast-like cells (BOLCs) [24].

During the last decades, the use of microcalcification patterns in radiological clinical practice has been the most important evaluation criterion for the early diagnosis of breast cancer.

Nevertheless, mammography alone is not sufficient to make a differential diagnosis and histological examinations are mandatory in order to characterize the type of breast lesion.

In this work, we introduce for the first time the use of EDX microanalysis technique as an additional instrumental approach to better characterize microcalcifications detected by mammography.

Our results suggest that EDX microanalysis, associated with the radiological exam of breast microcalcifications as well as histopathological data could provide useful information for the design of new imaging technologies able to discriminate microcalcifications in vivo, which would represent a significant step forward in noninvasive breast cancer screening.

Also, in line with previous data, we showed that breast lesions with microcalcifications are characterized by the presence of BOLCs expressing molecules typical of osteoblasts [7, 24]. Such cells could explain the formation of ectopic calcifications in breast lesions, especially when they are made of elements such as HA and Mg-Hap, which are particularly related to tumor malignancy. Finally, a better knowledge of the early signs of breast cancer, such as microcalcifications, paves the way for a deeper comprehension of the physio-pathological processes leading to breast cancer development.

Conclusions

Multidisciplinary and multimodal analysis of microcalcifications (e.g. mammography, EDX microanalysis, histology), could open new perspectives for the application of computational strategies aimed at the development of algorithms able to predict the risk of breast cancer occurrence. In this context, a more accurate knowledge of microcalcifications characteristics could not only help clinicians in the management of breast cancer patients, but also proposes the occurrence of ectopic calcification in mammary tissue as part of the tumorigenic process. In addition, the morphological and molecular characterization of BOLCs can lay the foundation for the comprehension of the biological basis about the formation of breast microcalcifications.

Acknowledgements This work was supported by FILAS Grant FILAS-SO-2011–1076 and OrchideaLab S.r.l. Authors thank Clara Nazaro, Harpreet Kaur Lamsira and Alessandro Polidori for technical support.

Compliance with Ethical Standards

Conflict of Interest There are no potential conflicts of interest relating to the manuscript, and there were no extramural sources supporting this research (excluding sources already declared). The study is original and the manuscript has not been published yet and is not being considered for publication elsewhere in any language either integrally or partially except as an abstract. All authors have agreed with the submission in its present (and subsequent) forms.

References

1. Mann S, Webb J, Williams RJP. Biomineralisation: chemical and biochemical perspectives. Ed. VCH Verlag. Weinheim, Germany; 1990.
2. Jemal A, SIiegel R, Ward E, Murray T, Xu J, Thun MJ. Cancer statistics, 2007. CA Cancer J Clin. 2007;57:43–66.
3. Ferranti C, Coopmans de Yoldi G, Biganzoli E, Bergonzi S, Mariani L, Scaperrotta G, et al. Relationships between age, mammographic features and pathological tumour characteristics in non-palpable breast cancer. Br J Radiol. 2000;73(871):698–705.
4. Gülsün M, Demirkazik FB, Ariyürek M. Evaluation of breast microcalcifications according to breast imaging reporting and data system criteria and Le Gal's classification. Eur J Radiol. 2003;47(3):227–31.
5. Lattanzio V, Simonetti G. Mammografia. Guida alla refertazione ed alla codifica dei risultati RE.CO.R.M. 2002 Napoli Idelson Gnocchi srl?
6. Haka AS, Shafer-Peltier KE, Fitzmaurice M, Crowe J, Dasari RR, Feld MS. Identifying differences in microcalcifications in benign and malignant breast lesions by probing differences in their chemical composition using Raman spectroscopy. Cancer Res. 2002;62(18):5375–80.
7. Scimeca M, Giannini E, Antonacci C, Pistolese CA, Spagnoli LG, Bonanno E. Microcalcifications in breast cancer: an active phenomenon mediated by epithelial cells with mesenchymal characteristics. BMC Cancer. 2014;14:286.

8. Radi MJ. Calcium oxalate crystals in breast biopsies. An overlooked form of microcalcification associated with benign breast disease. Arch Pathol Lab Med. 1989;113(12):1367–9.
9. Scimeca M, Bonfiglio R, Varone F, Ciuffa S, Mauriello A, Bonanno E. Calcifications in prostate cancer: an active phenomenon mediated by epithelial cells with osteoblast-phenotype. Microsc Res Tech. 2018; https://doi.org/10.1002/jemt.23031.
10. Rao AA, Feneis J, Lalonde C, Ojeda-Fournier H. A pictorial review of changes in the BI-RADS fifth edition. Radiographics. 2016;36(3):623–39.
11. Le Gal M, Chavanne G, Pellier D. Valeur diagnostique des microcalcifications groupees decouvertes par mammographies: a propos de 277 cas avec verification histologique et sans tumeur du sein palpable. Bull Cancer (Paris). 1984;71:57–64.
12. Simonetti G, Lattanzio V. Mammografia. Guida alla Refertazione e alla Codifica dei Risultati – Re.Co.R.M. Idelson-Gnocchi Editore 2002.
13. Tabár L, Tot T, Dean PB. Breast cancer: the art and science of early detection with mammography. Stuttgart: Thieme; 2005.
14. Fox CH, Johnson FB, Whiting J, Roller PP. Formaldehyde fixation. J Histochem Cytochem. 1985;33:845–53.
15. Tarantino U, Feola M, Celi M, Scimeca M. PTX3: a new mediator of bone metabolism and osteoporosis. Muscle, Ligaments and Tendons Journal. 2017;7(1):200–1. https://doi.org/10.11138/mltj/2017.7.1.200.
16. Scimeca M, Orlandi A, Terrenato I, Bischetti S, Bonanno E. Assessment of metal contaminants in non-small cell lung cancer by EDX microanalysis. Eur J Histochem. 2014;58:2403.
17. Scimeca M, Pietroiusti A, Milano F, Anemona L, Orlandi A, Marsella LT, et al. Elemental analysis of histological specimens: a method to unmask nano asbestos fibers. Eur J Histochem. 2016;60(1):2573.
18. Scimeca M, Bischetti S, Lamsira HK, Bonfiglio R, Bonanno E. Energy dispersive X-ray (EDX) microanalysis: a powerful tool in biomedical research and diagnosis. Eur J Histochem. 2018;62(1):2841.
19. Lakhani SR, Ellis IO, Schnitt SJ, Tan PH, van de Vijver MJ. WHO classification of tumours of the breast. 4th, vol. 4. France: IARC Press; Lyon; 2012. p. 34–8.
20. Scimeca M, Antonacci C, Bonanno E. Breast microcalcifications: a focus. J Cell Sci Ther. 2015;S8:e101.
21. Tabar L, Tony Chen HH, Amy Yen MF, Tot T, Tung TH, Chen LS, et al. Mammographic tumor features can predict long-term outcomes reliably in women with 1-14-mm invasive breast carcinoma. Cancer. 2004;101(8):1745–59.
22. Busin GC, Keppler U, Menges V. Differences in microcalcification in breast tumours. Virchows Arch A Pathol Anat Histopathol. 1981;393:303–7.
23. Cox RF, Hernandez-Santana A, Ramdass S, McMahon G, Harmey JH, Morgan MP. Microcalcifications in breast cancer: novel insights into the molecular. mechanism and functional consequence of mammary mineralisation. Br J Cancer. 2012;106(3):525–37.
24. Scimeca M, Antonacci C, Toschi N, Giannini E, Bonfiglio R, Buonomo CO, et al. Breast osteoblast-like cells: a reliable early marker for bone metastases from breast cancer. Clin Breast Cancer. 2017; pii: S1526-8209(17)30209-4
25. Scimeca M, Bonfiglio R, Montanaro M, Bonanno E. Osteoblast-like cells in human cancers: new cell type and reliable markers for bone metastasis. Future Oncol. 2018;14(1):9–11. https://doi.org/10.2217/fon-2017-0472.
26. Sánchez-Duffhues G, Hiepen C, Knaus P, Ten Dijke P. Bone morphogenetic protein signaling in bone homeostasis. Bone. 2015;80:43–59.
27. Scimeca M, Antonacci C, Colombo D, Bonfiglio R, Buonomo OC, Bonanno E. Emerging prognostic markers related to mesenchymal characteristics of poorly differentiated breast cancers. Tumour Biol. 2016;37(4):5427–35.
28. Scimeca M, Salustri A, Bonanno E, Nardozi D, Rao C, Piccirilli E, et al. Impairment of PTX3 expression in osteoblasts: a key element for osteoporosis. Cell Death Dis. 2017;8(10):e3125.
29. Lee EJ, Song DH, Kim YJ, Choi B, Chung YH, Kim SM, et al. PTX3 stimulates osteoclastogenesis by increasing osteoblast RANKL production. J Cell Physiol. 2014;229(11):1744–52.
30. Theoleyre S, Wittrant Y, Tat SK, Fortun Y, Redini F, Heymann D. The molecular triad OPG/RANK/RANKL: involvement in the orchestration of pathophysiological bone remodeling. Cytokine Growth Factor Rev. 2004;15(6):457–75.
31. Komori T. Regulation of osteoblast differentiation by Runx2. Adv Exp Med Biol. 2010;658:43–9. https://doi.org/10.1007/978-1-4419-1050-9_5.
32. Hunter GK. Role of osteopontin in modulation of hydroxyapatite formation. Calcif Tissue Int. 2013;93(4):348–54.